Almost all reported mutations of *IDH1/2* in gliomas are heterozygous missense affecting either codon 132 in *IDH1* or codon 172 in *IDH2* [11]. About 90 % of all *IDH1/2* mutations are c.395G>A (R132H) in *IDH1* [11]. Other *IDH1* mutations include c.394C>T (R132C), c.394C>A (R132S), c.394C>G (R132G), c.395G>T (R132L), R132P (nucleotide change not reported in the original article) and R132V (c.394C>G and c.395G>T); the latter two mutations reported only in single cases [9, 29]. *IDH2* c.515G>A (R172K) accounts for about 3 % of all *IDH1/2* mutations, and other *IDH2* mutations include c.515G>T (R172M), c.514A>T (R172W), c.516G>C (R172S) and c.514A>G (R172G) [11].

Direct sequencing and immunohistochemistry (IHC) are the most widely used methods for assessing the *IDH1/2* status. Sanger sequencing, however, has the limitation of being unable to detect mutations in tumor samples that contain extensive necrosis or are contaminated with non-neoplastic cells; the accuracy of Sanger sequencing, therefore, largely depends on the quality of the sample [1, 5]. For IHC, two specific antibodies for the mutant R132H, DIA-H09 and IMab-1, are commercially available and well-characterized [4, 15]. The significant advantage that IHC has over Sanger sequencing is that FFPE samples are readily available through routine histopathological examination. IHC, however, can only detect the mutation specific to the antibody used. Antibodies specific for mutations other than R132H have also been developed [14, 16], however, their efficacy needs to be further validated in clinic.

We have developed rapid and robust assays for the detection of *IDH1/2* mutations using pyrosequencing, which is a sequence-by-synthesis technique based on the luciferase–luciferin light release as a signal for nucleotide incorporation into target DNA [24]. Our novel assays enable the detection of all reported mutations in *IDH1* or *IDH2* at a single run for each gene. We describe the details of our original assay and evaluate its potential efficacy in clinical application.

Materials and methods

DNA samples

Frozen tissue samples from a total of 160 glioma cases operated at the National Cancer Center Hospital (Tokyo, Japan) were included in this study; 29 diffuse astrocytomas, 11 oligoastrocytomas, 2 oligodendrogliomas, 28 anaplastic astrocytomas, 21 anaplastic oligoastrocytomas, 8 anaplastic oligodendrogliomas, 55 primary glioblastomas and 6 secondary glioblastomas. Matched FFPE samples were available for analysis in nineteen cases (Supplementary Table 1). Twenty blood samples were also analyzed as a normal control. The study was approved by the local institutional review board. Histological diagnoses were made according to the WHO classification [18]. A DNeasy Blood & Tissue Kit (Qiagen, Tokyo, Japan) was used to extract DNA.

Control plasmids

All control plasmids that contain every single type of mutation except *IDH1* R132L (see below) were generated by subcloning the mutated sequences from the tumor samples (obtained from the Department of Pathology, University of Cambridge [12]). Briefly, after amplifying the genomic DNA containing the different types of *IDH1/2* mutation, the polymerase chain reaction (PCR) product was subcloned into the pMD20-T vector by a TA cloning procedure using the 10X A-Attachment mix (TOYOBO, Osaka, Japan) and a Mighty Cloning Kit (TAKARA Bio Inc., Tokyo, Japan) according to the manufacturers' recommendations. The control plasmids for R132H, R132C, R132S and R132G in *IDH1*, and R172K, R172M, R172W and R172S in *IDH2* were all generated using the method described above. The plasmid containing the *IDH1* R132L (c.395G>T) mutation was generated by site-directed mutagenesis because no samples in our tumor cohort had this mutation. For this procedure, 50 ng of plasmids with wild-type *IDH1* were unidirectionally amplified using a complementary pair of oligonucleotides containing the mutation, and the non-mutant *dam*-methylated template plasmid DNA was digested using the DpnI restriction enzyme (New England Biolabs Japan Inc., Tokyo, Japan) before the newly synthesized mutated construct is transformed into *E. coli*.

Pyrosequencing

Polymerase chain reaction primers were designed for amplifying relatively small DNA fragments, either 86 bp for *IDH1* or 85 bp for *IDH2* sequences, containing the targeted region so that the assay could potentially be used for DNA extracted from archival tissues. Detailed information about the primers is given in Table 1. Templates for pyrosequencing were prepared by amplifying genomic DNA (10 ng) with primers that were biotinylated for the template strands. The 25 μl PCR mix included 62.5 μM of each dNTP, 0.625 units of Ampli Taq Gold 360 DNA polymerase and 0.5 μM of primers for *IDH1/2* each as per manufacturer's recommendations. The $MgCl_2$ concentration of the PCR mix was optimized for each primer set; 2 mM for *IDH1* and 1.5 mM for *IDH2*. The thermal cycling conditions for amplification were as follows: one cycle of initial denaturation at 95 °C for 10 min, followed

Table 1 Sequences of the primers for PCR for pyrosequencing, Sanger sequencing, and the pyrosequencing assays

Procedure	Sequence
PCR for pyrosequencing	
For *IDH1* (product length 86 bp)	
Forward primer (PC6041)	CAAAAATATCCCCCGGCTTG
Reverse primer (PC6042)	bio-CAACATGACTTACTTGATCCCC
For *IDH2* (product length 85 bp)	
Forward primer (PC6099)	ACATCCCACGCCTAGTCCC
Reverse primer (PC6100)	bio-TCTCCACCCTGGCCTACCTG
Pyrosequencing	
For *IDH1*	
Primer (P0125)	ACCTATCATCATAGGT
Sequence to analyze	CDTCATGCTTAT
Dispensation order	GATCATGTCATG
Assay type	AQ assay
For *IDH2*	
Primer (P0126)	CCCATCACCATTGGC
Sequence to analyze	ANGCAC
Dispensation order	TATGTCACGCAC
Assay type	AQ assay
Sanger sequencing [10]	
For *IDH1* (product length 254 bp)	
Forward primer (IDH1 fc)	ACCAAATGGCACCATACGA
Reverse primer (IDH1 rc)	TTCATACCTTGCTTAATGGGTGT
For *IDH2* (product length 293 bp)	
Forward primer (IDH2 fc)	GCTGCAGTGGGACCACTATT
Reverse primer (IDH2 rc)	TGTGGCCTTGTACTGCAGAG

by 35 cycles 95 °C 30 s, 55 °C 30 s, and 72 °C 30 s. An additional cycle at 72 °C for 5 min was added to complete the elongation step. Amplification of the PCR products was confirmed by running 3 μl of the reaction mix on an agarose gel.

Single-stranded templates for pyrosequencing were prepared as per manufacturer's recommendations using 20 μl of PCR template (Qiagen, Tokyo, Japan). The purified single-stranded PCR products were denatured and annealed to 15 pmol of pyrosequencing primer. Pyrosequencing was performed using the PyroGold Q96 SQA Reagents and the PyroMark Q96 software (version 2.5.7) on a PSQ96 pyrosequencer (Qiagen, Tokyo, Japan) according to the manufacturer's recommendations. The data were analyzed using the PyroMark Q96 software. The 3′ end of the pyrosequencing primers was designed immediately upstream of each hotspot. The dispensation orders for pyrosequencing were designed so that all possible mutations at the first two positions of codon 132 of *IDH1* and codon 172 of *IDH2* could be identified in a single assay for each gene (indicated in Table 1). An AQ analysis, which is an analysis mode within the PyroMark Q96 software, was performed so that the percentage of mutant allele could be quantified in this assay.

Sanger sequencing

Templates for Sanger sequencing were prepared by amplifying 10 ng of genomic DNA with a set of primers (Table 1). The 10 μl PCR mix included 2.0 mM of $MgCl_2$, 125 μM of each dNTP, 0.5 units of Ampli Taq Gold 360 DNA polymerase (Applied Biosystems, Foster City, CA, USA) and 0.5 μM of primer pairs (IDH1 fc and rc for *IDH1*, or IDH2 fc and rc for *IDH2* [10]). The same primer pair as the one used for *IDH1* pyrosequencing (PC6041 and PC6042) was used in a single FFPE sample (DA068) which was not sufficiently amplified by the standard primer pairs for Sanger. The thermal cycling for amplification was as follows: one cycle of initial denaturation at 95 °C for 10 min, followed by 40 cycles of 95 °C 30 s, 55 °C 30 s, 72 °C 30 s with an additional cycle of 72 °C for 7 min. Amplification of the 254 bp (*IDH1*) or 293 bp (*IDH2*) product was confirmed by running 3 μl of the reaction mix on an agarose gel. After purification using ExoSAP (Affymetrix Japan KK, Tokyo, Japan) as per manufacturer's recommendations, cycle sequencing was carried out using the BigDye Terminator v3.1 cycle sequencing kit (Applied Biosystems, Foster City, CA, USA) and the same forward primer (IDH1 fc, PC6041 or IDH2 fc) as the amplification of genomic DNA.

The thermal cycling for amplification was as follows: 25 cycles of 96 °C 10 s, 50 °C 15 s, and 60 °C 4 min.

Immunohistochemistry

Immunohistochemistry using a mouse monoclonal anti-human IDH1 R132H antibody (H09, Dianova, Hamburg, Germany) was performed by a polymeric method of EnVision FLEX system (Dako Japan Inc, Tokyo, Japan) with an automatic staining machine (Auto-stainer Link 48, Dako Japan Inc, Tokyo, Japan) as previously reported [8]. The presence of positive granular cytoplasmic staining in the tumor cells was judged as being indicative of mutant *IDH1*.

Results

The sensitivity and specificity of the newly developed pyrosequencing assays for *IDH1* and *IDH2* mutation

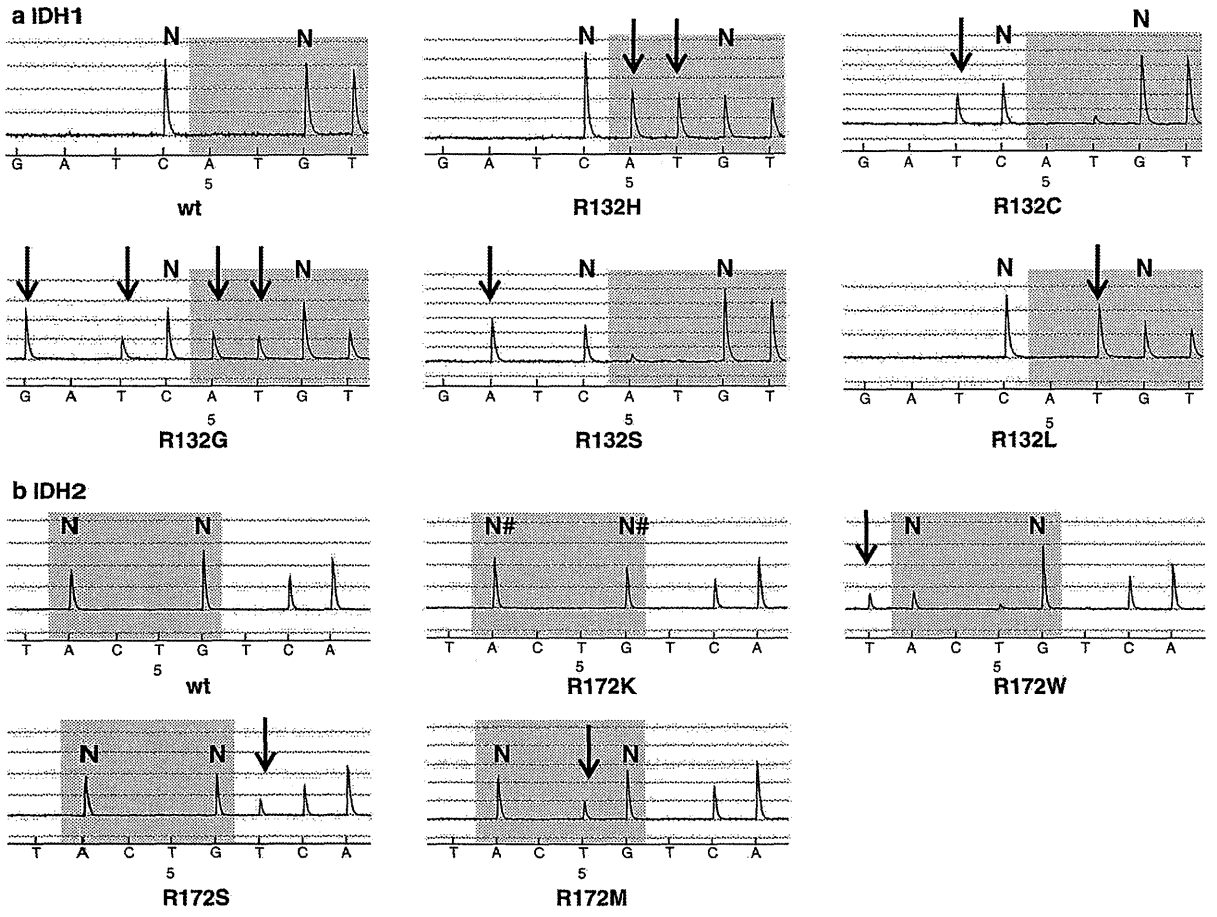

Fig. 1 Pyrograms for each *IDH1/2* mutation. Samples containing equal amounts of wild-type and mutant DNA were subjected to the pyrosequencing assays. The pyrograms show the mutation-specific pattern obtained for each mutation in *IDH1* (**a**) or *IDH2* (**b**) indicated by the *arrows*. "N" denotes the normal peaks. In this assay, all the mutations but *IDH2* R172K have their specific patterns of peaks which are not present in the wild-type samples. The *IDH2* R172K mutation is detected as a higher peak at the 3rd dispensation (*A*) and a lower peak at the 6th dispensation (*G*); those peaks are marked by "N#"

screening were first validated using the control DNA mixture that contains equal amounts of the wild-type and mutated plasmid constructs. All *IDH1* mutations were successfully identified by detecting mutant-specific peaks in a single assay. As shown in Fig. 1a, only one peak at the 4th dispensation (C) was observed among the first 5 dispensations in the pyrogram of the wild-type *IDH1*, while abnormal peaks were observed either at the 1st, 2nd, 3rd, 5th or 6th dispensation only in the mutated DNA, but not in the wild type. As for *IDH2*, two peaks at the 3rd (A) and 6th (G) dispensations were observed in the pyrogram of the wild type, while abnormal peaks unique to each mutation were observed at the 2nd, 5th and 7th dispensations in R172W, R172M and R172S mutants, respectively (Fig. 1b). The *IDH2* R172K mutation could be detected by a peak twice as high as the wild type at the 3rd dispensation and a peak half as high as the wild type at the 6th dispensation. Thus, our assays identify all mutants of *IDH1/2*, except the R172K mutant, by the presence of abnormal peaks which should be absent in the wild-type *IDH2*. The R172K mutation can also be detected by quantifying the mutant allele frequency using an AQ analysis as described below.

Twenty blood samples were then subjected to pyrosequencing to determine the threshold of normal variation. For the c.395 position of *IDH1*, the mean frequency of A, T, G (wild type) and C was 0 %, 0.078 ± 0.065 % (range 0–0.27 %), 99.9 ± 0.1 % (range 99.7–100 %) and 0 %, respectively. For the c.514 position of *IDH2*, the mean frequency of A, T, G (wild type) and C was 7.0 ± 2.6 % (range 3.6–13.9 %), 0 %, 93.0 ± 2.6 % (range 86.1–96.4 %) and 0 %, respectively. Based on the

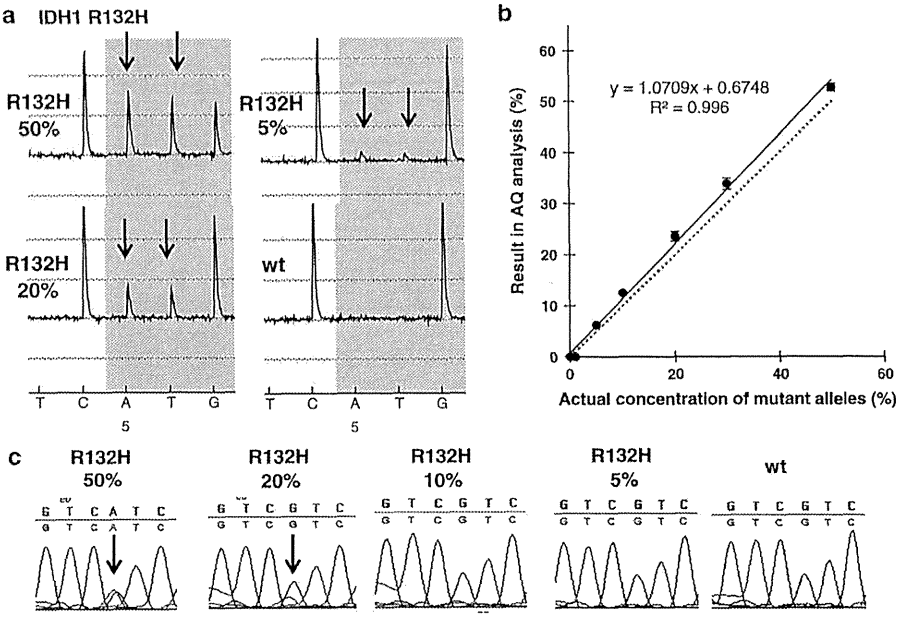

Fig. 2 Serial dilution analysis for the evaluation of the sensitivity in detecting R132H mutation in *IDH1*. **a** A mixture of the control plasmid constructs containing variable ratios of wild-type and R132H mutant alleles of *IDH1* was subjected to pyrosequencing. Even 5 % of mutant allele could be detected as a peak as shown in the pyrogram (the mutated peaks are indicated by *arrows*). **b** The triplicated results of the pyrosequencing assay plotted against the expected concentration showing a very high concordance ($R^2 = 0.996$). **c** The peak of the mutant allele in the Sanger sequencing chromatogram was obscure in samples containing 10 % or less mutant DNA

maximum error ratio in the normal blood controls, the mutant allele frequency of 0.27 % or less for *IDH1* and 13.9 % or less for *IDH2* will be considered as within normal variation.

Next, serial dilution experiments were performed to assess the sensitivity of the pyrosequencing assay to detect *IDH1/2* mutations. Pyrosequencing and Sanger sequencing were performed on either R132H of *IDH1* or R172K of *IDH2* mutant construct serially diluted with the wild-type plasmid to achieve ratios of mutant DNA of 0, 1, 5, 10, 20, 30 or 50 % in triplicate as follows. The presence of the *IDH1* R132H mutant allele was detected as a clearly distinct peak in the pyrogram in samples containing 5 % or more mutant DNA (Fig. 2a) whereas the mutant peak in the chromatograms obtained from direct sequencing was apparent only in samples with 20 % or more mutant DNA (Fig. 2c). The mean measured frequencies of the triplicate experiments showed a strong linear correlation, being almost equal to the actual frequencies of the mutant alleles ($R^2 = 0.996, p < 0.0001$) (Fig. 2b). Based on the threshold defined in the above experiments, the samples showing a mutant allele ratio of 5 % or more were judged to be mutated in this assay. This sensitivity was remarkably comparable with the value found in previously reported assays [7, 26]. As for R172K in *IDH2*, because it was not possible to design an assay to detect the mutation by the presence of a unique peak, this mutation could nevertheless be characterized by quantifying the peak common to wild-type and mutated alleles using the AQ analysis. The mean frequencies of triplicate experiments were slightly higher, nonetheless strongly correlated with the expected frequencies of the mutant alleles ([Percentage in AQ analysis] = 1.07 * [Actual percentage] +4.13, $R^2 = 0.998, p < 0.0001$) (Fig. 3b). Based on the results of the blood samples, the samples showing a mutant allele concentration of 10 % or above were considered as mutated in this assay. In Sanger sequencing, the mutant allele could only be detected in samples containing at least 10 % of the mutated DNA (Fig. 3c).

Finally, the pyrosequencing assay and Sanger sequencing were compared in a series of glioma samples to validate the efficacy of detecting mutations on genuine clinical cases. *IDH1* was Sanger sequenced in all 160 cases and *IDH2* in selected cases mainly consisted of those without *IDH1* mutations ($n = 113$). The result of each case is shown in Supplementary Table 1. The pyrosequencing-based analysis for *IDH1* detected mutations in 75 cases (74 cases with R132H and a single case with R132S), while the Sanger sequencing failed to detect three R132H mutant cases (DA068, AA067 and OA 040). The frequencies of mutant alleles measured by pyrosequencing were low in the three discordant cases (10.8–16.2 %), suggesting that those samples contained a low percentage of tumor cells. The results of the pyrosequencing and Sanger sequencing screening for *IDH2*, which identified R172K mutations in 4 tumors (Supplementary Table 1), were identical in all cases analyzed.

Immunohistochemistry was performed on 69 cases including the three discordant cases between Sanger sequencing and pyrosequencing. IHC and pyrosequencing results were concordant in all cases. To ensure that exactly the same specimen was used for comparison, the three

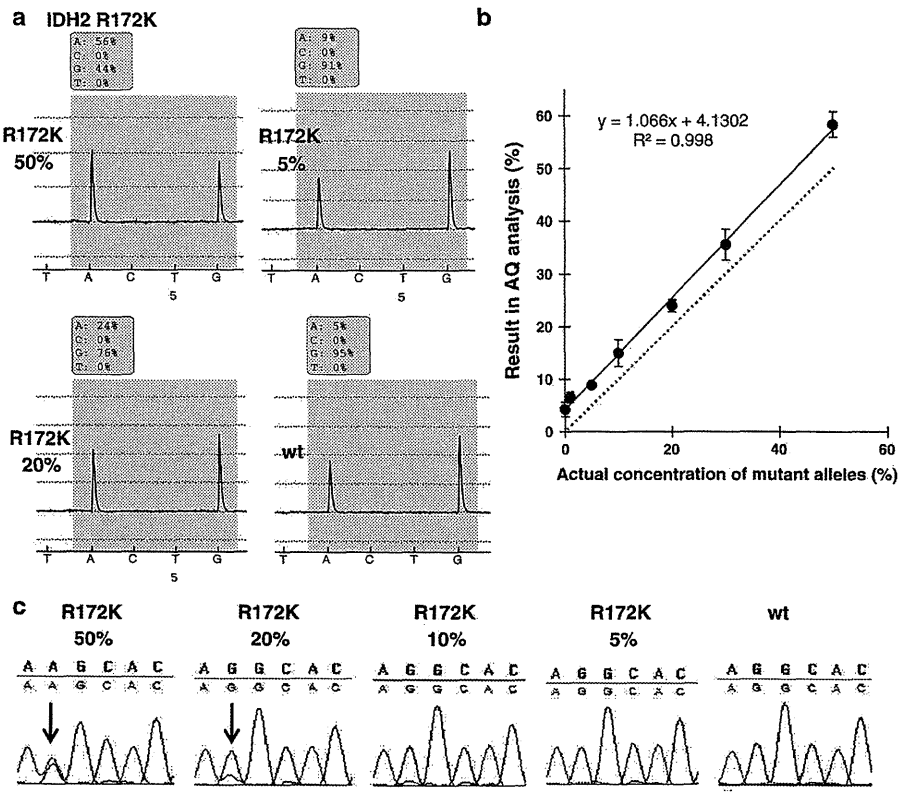

Fig. 3 Serial dilution analysis for the evaluation of the sensitivity in detecting R172K mutation in *IDH2*. **a** Samples containing variable concentrations of wild-type and R172K mutant alleles of *IDH2* were subjected to pyrosequencing. For detection of this mutation, the assessment was based on the allele ratio calculated by the AQ assay as shown in the *insets*. **b** The pyrosequencing assay gives slightly higher values, nonetheless it showed a high concordance with the expected concentration. **c** The peak of mutant allele in the Sanger sequencing (*arrows*) was obscure in samples containing 10 % or less mutant DNA

discordant cases between pyrosequencing and Sanger sequencing (DA068, AA067 and OA 040) were subjected to a new round of Sanger sequencing and pyrosequencing using DNA extracted from sequentially sectioned FFPE samples which were used for IHC. In one of the three previously discordant cases (DA068), the R132H mutation in *IDH1* was detected by pyrosequencing and IHC, but not by Sanger sequencing (Fig. 4). In the other two previously discordant cases (AA067 and OA040), the IHC was found positive and the repeated Sanger sequencing also confirmed the presence of the mutations as a minor allele.

To test whether pyrosequencing is applicable to FFPE, the DNAs extracted from a further 16 matched FFPE specimens were subjected to pyrosequencing for *IDH1*. The results from FFPE and frozen samples were consistent in all cases examined (Supplementary Table 1).

Discussion

The purpose of this paper is to present and discuss in detail a novel pyrosequencing assay for the mutational analysis of *IDH1/2*. This protocol was specifically designed with the clinical setting in mind and should, therefore, be quickly and easily implemented in any laboratories equipped with a pyrosequencer. The assay is fully compatible with Sanger sequencing and shown to be robust, efficient and more sensitive in detecting low-level mutations than the Sanger sequencing method. This assay is particularly useful for the genetic screening of *IDH1/2* mutations in a large tumor cohort as exemplified by its successful application in our recent study of gliomas [2].

Pyrosequencing has been applied to various genetic analyses including mutation detection at hotspots in *KRAS*, or quantitative measurement of methylation levels in the CpG island of the O^6-Methylguanine-DNA methyltransferase (*MGMT*) gene using bisulfite-modified DNA [19, 21, 23]. Several previous studies have also reported the use of pyrosequencing for the detection of *IDH1/2* mutations [6, 7, 17, 20, 26, 27, 32]. These studies mainly focused on the feasibility of detecting *IDH1/2* mutations by pyrosequencing or the clinical significance of these mutations, however, full details of the assay were not given, which prevented independent validation of the assay by others [6, 7, 20, 27, 32]. Our novel pyrosequencing assays for detecting *IDH1/2* mutations are fully validated using engineered controls for almost all known *IDH1* R132 and *IDH2* R172 mutations. We also strived to provide all the technical details to allow an immediate replication of the technique. The robustness of a pyrosequencing-based

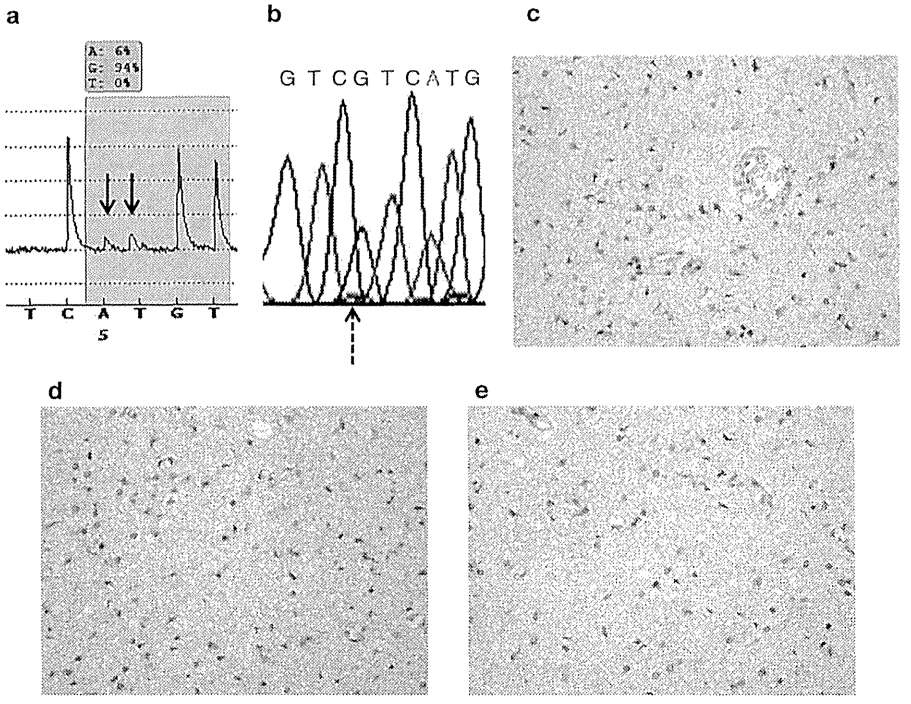

Fig. 4 The discordant case. A single case (DA068) showed discordance between pyrosequencing, Sanger sequencing and immunohistochemistry for *IDH1*. **a** The peaks indicating the R132H mutation (*arrows*) are shown in the pyrogram. The ratio of the mutant alleles was calculated to be 6.48 % by the AQ assay, suggesting the low density of tumor cells in this specimen. **b** A peak of adenine (*green*) at the hotspot (*broken arrow*) indicating the R132H mutation was obscure and hard to distinguish from non-specific peaks in the chromatogram. The cytoplasm of infiltrating tumor cells was positively stained in IHC using an antibody against the R132H mutation (original magnification ×400). The overall tumor cell content of this FFPE sample was low. Three separate areas with different tumor cell contents are shown (**c** the highest in this specimen, **d** intermediate, **e** low)

analysis depends on the design of the dispensation order, which determines the various types of mutation detectable by the assay. We successfully detected virtually all types of the known reported *IDH1/2* mutations using a single assay each for *IDH1* and 2. Some of the previous studies applied more than one assay for this purpose [26]. Moreover, all mutations except one, *IDH2* R172K, are detected by the presence of mutation-specific peaks which are absent in the wild-type samples, making the assay highly sensitive. Not enough detailed information such as the dispensation order for example was provided in other previous studies [17]. With our novel assay, we set to achieve a fast and easy implementation aimed at the clinical setting.

We demonstrated the sensitivity and quantitativity of our assays by serial dilution analysis. It is a known fact that the sensitivity of conventional Sanger sequencing may be compromised by contamination of the samples with non-neoplastic tissues. Our results suggest that the conventional Sanger technique requires the presence of at least 20 % of the mutant alleles for the detection to be reliable [29]. By contrast, our assay detects as little as 5 % of the mutant alleles, and this sensitivity is comparable to previous studies [7, 26]. Glioma tissues often have a heterogeneous cell contents due to the invasive nature of the tumor into the surrounding brain tissue as well as its tendency to attract microglia infiltration [22]. The detection of *IDH1/2* mutations in samples containing a low percentage of tumor cells is challenging, but it is an absolute necessity for its clinical application. We showed that our pyrosequencing assays were applicable to FFPE samples, which are consistent with previous reports [6, 7, 26].

An optimal method for *IDH1/2* mutation testing remains under debate [28]. Some studies found that the results obtained by pyrosequencing were identical to those generated by Sanger sequencing [7, 26]. One study reported comparable frequencies of *IDH1/2* mutations detected between pyrosequencing, Sanger sequencing and IHC [17]. In the present study, the result of IHC was identical to that of pyrosequencing, while Sanger sequencing failed to detect mutations in three cases (4 % of *IDH1* mutated cases). The discordance between pyrosequencing and Sanger sequencing was attributable to the low tumor contents in each sample (see "Results"). Pyrosequencing thus provides higher sensitivity, robustness and throughput for

the analysis of *IDH1/2* mutation than Sanger sequencing [7]. Although the consistency between pyrosequencing and IHC needs further validation, pyrosequencing enables rapid screening for *IDH1/2* mutations (about 3–4 h) in a setting where DNA samples are already extracted. Ultimately, the optimal method for *IDH1/2* testing also depends on criteria such as the purpose of each study and/or the types of specimens available.

In summary, we have established a robust and sensitive assay for the detection of *IDH1/2* mutations. Our pyrosequencing assays are suitable for the analysis of a large number of samples, particularly if the samples are all simultaneously investigated such as in a large-scale retrospective clinical study.

Acknowledgments The authors thank Dr. Sylvia Kocialkowski for critical reading of the manuscript. This work was supported by JSPS KAKENHI Grant Numbers 24659650 (H. A.), 25462283 (K. I.) and by the National Cancer Center Research and Development Fund 23-A-50 (K. I.).

References

1. Agarwal S, Sharma MC, Jha P, Pathak P, Suri V, Sarkar C, Chosdol K, Suri A, Kale SS, Mahapatra AK (2013) Comparative study of IDH1 mutations in gliomas by immunohistochemistry and DNA sequencing. Neuro Oncol 15:718–726
2. Arita H, Narita Y, Fukushima S, Tateishi K, Matsushita Y, Yoshida A, Miyakita Y, Ohno M, Collins VP, Kawahara N, Shibui S, Ichimura K (2013) Upregulating mutations in the TERT promoter commonly occur in adult malignant gliomas and are strongly associated with total 1p19q loss. Acta Neuropathol 126:267–276
3. Balss J, Meyer J, Mueller W, Korshunov A, Hartmann C, von Deimling A (2008) Analysis of the IDH1 codon 132 mutation in brain tumors. Acta Neuropathol 116:597–602
4. Capper D, Zentgraf H, Balss J, Hartmann C, von Deimling A (2009) Monoclonal antibody specific for IDH1 R132H mutation. Acta Neuropathol 118:599–601
5. Choi J, Lee EY, Shin KJ, Minn YK, Kim J, Kim SH (2013) IDH1 mutation analysis in low cellularity specimen: a limitation of diagnostic accuracy and a proposal for the diagnostic procedure. Pathol Res Pract 209:284–290
6. Cykowski MD, Allen RA, Fung KM, Harmon MA, Dunn ST (2012) Pyrosequencing of IDH1 and IDH2 mutations in brain tumors and non-neoplastic conditions. Diagn Mol Pathol 21:214–220
7. Felsberg J, Wolter M, Seul H, Friedensdorf B, Goppert M, Sabel MC, Reifenberger G (2010) Rapid and sensitive assessment of the IDH1 and IDH2 mutation status in cerebral gliomas based on DNA pyrosequencing. Acta Neuropathol 119:501–507
8. Fukushima S, Narita Y, Miyakita Y, Ohno M, Takizawa T, Takusagawa Y, Mori M, Ichimura K, Tsuda H, Shibui S (2013) A case of more than 20 years survival with glioblastoma, and development of cavernous angioma as a delayed complication of radiotherapy. Neuropathology 33:576–581
9. Gravendeel LA, Kloosterhof NK, Bralten LB, van Marion R, Dubbink HJ, Dinjens W, Bleeker FE, Hoogenraad CC, Michiels E, Kros JM, van den Bent M, Smitt PA, French PJ (2010) Segregation of non-p.R132H mutations in IDH1 in distinct molecular subtypes of glioma. Hum Mutat 31:E1186–E1199
10. Hartmann C, Meyer J, Balss J, Capper D, Mueller W, Christians A, Felsberg J, Wolter M, Mawrin C, Wick W, Weller M, Herold-Mende C, Unterberg A, Jeuken JW, Wesseling P, Reifenberger G, von Deimling A (2009) Type and frequency of IDH1 and IDH2 mutations are related to astrocytic and oligodendroglial differentiation and age: a study of 1,010 diffuse gliomas. Acta Neuropathol 118:469–474
11. Horbinski C (2013) What do we know about IDH1/2 mutations so far, and how do we use it? Acta Neuropathol 125:621–636
12. Ichimura K, Pearson DM, Kocialkowski S, Backlund LM, Chan R, Jones DT, Collins VP (2009) IDH1 mutations are present in the majority of common adult gliomas but rare in primary glioblastomas. Neuro Oncol 11:341–347
13. Johnson BE, Mazor T, Hong C, Barnes M, Aihara K, McLean CY, Fouse SD, Yamamoto S, Ueda H, Tatsuno K, Asthana S, Jalbert LE, Nelson SJ, Bollen AW, Gustafson WC, Charron E, Weiss WA, Smirnov IV, Song JS, Olshen AB, Cha S, Zhao Y, Moore RA, Mungall AJ, Jones SJ, Hirst M, Marra MA, Saito N, Aburatani H, Mukasa A, Berger MS, Chang SM, Taylor BS, Costello JF (2014) Mutational analysis reveals the origin and therapy-driven evolution of recurrent glioma. Science 343:189–193
14. Kaneko MK, Morita S, Tsujimoto Y, Yanagiya R, Nasu K, Sasaki H, Hozumi Y, Goto K, Natsume A, Watanabe M, Kumabe T, Takano S, Kato Y (2013) Establishment of novel monoclonal antibodies KMab-1 and MMab-1 specific for IDH2 mutations. Biochem Biophys Res Commun 432:40–45
15. Kato Y, Jin G, Kuan CT, McLendon RE, Yan H, Bigner DD (2009) A monoclonal antibody IMab-1 specifically recognizes IDH1R132H, the most common glioma-derived mutation. Biochem Biophys Res Commun 390:547–551
16. Kato Y, Natsume A, Kaneko MK (2013) A novel monoclonal antibody GMab-m1 specifically recognizes IDH1-R132G mutation. Biochem Biophys Res Commun 432:564–567
17. Lee D, Suh YL, Kang SY, Park TI, Jeong JY, Kim SH (2013) IDH1 mutations in oligodendroglial tumors: comparative analysis of direct sequencing, pyrosequencing, immunohistochemistry, nested PCR and PNA-mediated clamping PCR. Brain Pathol 23(3):285–293
18. Louis DN, Ohgaki H, Wiestler OD, Cavenee WK, Burger PC, Jouvet A, Scheithauer BW, Kleihues P (2007) The 2007 WHO classification of tumours of the central nervous system. Acta Neuropathol 114:97–109
19. Malley DS, Hamoudi RA, Kocialkowski S, Pearson DM, Collins VP, Ichimura K (2011) A distinct region of the MGMT CpG island critical for transcriptional regulation is preferentially methylated in glioblastoma cells and xenografts. Acta Neuropathol 121:651–661
20. Mascelli S, Raso A, Biassoni R, Severino M, Sak K, Joost K, Milanaccio C, Barra S, Grillo-Ruggieri F, Vanni I, Consales A, Cama A, Capra V, Nozza P, Garre ML (2012) Analysis of NADP+ -dependent isocitrate dehydrogenase-1/2 gene mutations in pediatric brain tumors: report of a secondary anaplastic astrocytoma carrying the IDH1 mutation. J Neurooncol 109:477–484
21. Mikeska T, Bock C, El-Maarri O, Hubner A, Ehrentraut D, Schramm J, Felsberg J, Kahl P, Buttner R, Pietsch T, Waha A (2007) Optimization of quantitative MGMT promoter methylation analysis using pyrosequencing and combined bisulfite restriction analysis. J Mol Diagn 9:368–381
22. Morimura T, Neuchrist C, Kitz K, Budka H, Scheiner O, Kraft D, Lassmann H (1990) Monocyte subpopulations in human gliomas: expression of Fc and complement receptors and correlation with tumor proliferation. Acta Neuropathol 80:287–294

23. Ogino S, Kawasaki T, Brahmandam M, Yan L, Cantor M, Namgyal C, Mino-Kenudson M, Lauwers GY, Loda M, Fuchs CS (2005) Sensitive sequencing method for KRAS mutation detection by Pyrosequencing. J Mol Diagn 7:413–421
24. Ronaghi M, Uhlen M, Nyren P (1998) A sequencing method based on real-time pyrophosphate. Science 281(363):365
25. Sanson M, Marie Y, Paris S, Idbaih A, Laffaire J, Ducray F, El Hallani S, Boisselier B, Mokhtari K, Hoang-Xuan K, Delattre JY (2009) Isocitrate dehydrogenase 1 codon 132 mutation is an important prognostic biomarker in gliomas. J Clin Oncol 27:4150–4154
26. Setty P, Hammes J, Rothamel T, Vladimirova V, Kramm CM, Pietsch T, Waha A (2010) A pyrosequencing-based assay for the rapid detection of IDH1 mutations in clinical samples. J Mol Diagn 12:750–756
27. Thon N, Eigenbrod S, Kreth S, Lutz J, Tonn JC, Kretzschmar H, Peraud A, Kreth FW (2012) IDH1 mutations in grade II astrocytomas are associated with unfavorable progression-free survival and prolonged postrecurrence survival. Cancer 118:452–460
28. van den Bent MJ, Hartmann C, Preusser M, Strobel T, Dubbink HJ, Kros JM, von Deimling A, Boisselier B, Sanson M, Halling KC, Diefes KL, Aldape K, Giannini C (2013) Interlaboratory comparison of IDH mutation detection. J Neurooncol 112:173–178
29. von Deimling A, Korshunov A, Hartmann C (2011) The next generation of glioma biomarkers: MGMT methylation, BRAF fusions and IDH1 mutations. Brain Pathol 21:74–87
30. Watanabe T, Nobusawa S, Kleihues P, Ohgaki H (2009) IDH1 mutations are early events in the development of astrocytomas and oligodendrogliomas. Am J Pathol 174:1149–1153
31. Yan H, Parsons DW, Jin G, McLendon R, Rasheed BA, Yuan W, Kos I, Batinic-Haberle I, Jones S, Riggins GJ, Friedman H, Friedman A, Reardon D, Herndon J, Kinzler KW, Velculescu VE, Vogelstein B, Bigner DD (2009) IDH1 and IDH2 mutations in gliomas. N Engl J Med 360:765–773
32. Yan W, Zhang W, You G, Bao Z, Wang Y, Liu Y, Kang C, You Y, Wang L, Jiang T (2012) Correlation of IDH1 mutation with clinicopathologic factors and prognosis in primary glioblastoma: a report of 118 patients from China. PLoS ONE 7:e30339

J Neurooncol (2014) 116:145–152
DOI 10.1007/s11060-013-1273-5

CLINICAL STUDY

Risk factors for early death after surgery in patients with brain metastases: reevaluation of the indications for and role of surgery

Hideyuki Arita · Yoshitaka Narita · Yasuji Miyakita · Makoto Ohno · Minako Sumi · Soichiro Shibui

Received: 4 April 2013 / Accepted: 9 October 2013 / Published online: 25 October 2013

Abstract Surgical resection remains an important option for the treatment of brain metastases despite recent advancements in radiotherapy and systemic therapy. When selecting surgical candidates, it is important to exclude terminal cases who will receive neither a survival benefit nor an improvement in their quality of life. We reviewed a total of 264 surgical cases of brain metastases and analyzed the clinical characteristics of early death in order to clarify the indication for and the role of surgery. The median survival time (MST) after surgery in all cases was 12.4 months. Early death was defined as death within 6 months, and 23 % (62 cases) of this series were succumbed to this. A decrease in postoperative Karnofsky performance status (KPS) (<70) ($P = 0.041$), lack of systemic therapy after surgery ($P < 0.0001$), and uncontrolled extracranial malignancies ($P = 0.0022$) were significantly related to early death in multivariate analysis, while preoperative KPS (<70) and recursive partitioning analysis (RPA) class were related to early death only in univariate analysis ($P < 0.05$). When analyzing patients with uncontrolled extracranial malignancies and those with a postoperative KPS score of 70 or greater (who were generally candidates for systemic therapy), the MST was significantly longer in the systemic therapy (+) group compared with the systemic therapy (−) group (12.5 vs. 5.6 months; $P = 0.0026$). Our data indicate that the postoperative RPA class and treatment strategy were associated with early death. Deterioration of patients by surgery should be avoided in the treatment of brain metastases.

Keywords Brain metastases · Surgery · Early death · Leptomeningeal metastases

Electronic supplementary material The online version of this article (doi:10.1007/s11060-013-1273-5) contains supplementary material, which is available to authorized users.

H. Arita · Y. Narita (✉) · Y. Miyakita · M. Ohno · S. Shibui
Department of Neurosurgery and Neuro-Oncology, National Cancer Center Hospital, 5-1-1, Tsukiji, Chuo-ku, Tokyo 104-0045, Japan
e-mail: yonarita@ncc.go.jp

M. Sumi
Department of Radiation Oncology, National Cancer Center, 5-1-1, Tsukiji, Chuo-ku, Tokyo 104-0045, Japan

Introduction

Brain metastasis is a life-threatening event for cancer patients and indicates that cancer has reached the advanced stages. Surgical resection remains an important option for treatment despite recent advancements in radiotherapy and chemotherapy. The aims of surgical resection are mass reduction and rapid improvement of neurological status.

Knowledge regarding the prognosis of extracranial lesions is important when making decisions about surgery. Several studies have attempted to identify prognostic factors, and various classification systems including recursive partitioning analysis (RPA) classification and graded prognostic assessment (GPA) have been developed [1, 2]. These classification systems have mainly been validated in patient populations treated with radiotherapy; however, some reports have indicated that these systems are useful for predicting survival time after surgery [3–9]. Considering the risks associated with treatment, terminal cases who receive neither a survival benefit nor an improvement in their quality of life (QOL) should be excluded during the selection of surgical candidates.

Herein, we describe a retrospective analysis of the relationship between clinical characteristics and the

outcome of surgery for brain metastases, and we discuss the indications for and the role of surgery.

Materials and methods

Patients

In total, we included 264 cases (156 men and 108 women) who underwent resection as their first surgery for brain metastases at the National Cancer Center Hospital in Japan between January 2000 and December 2011. The mean age of the included patients was 57.5 years (range 19–87), and their clinical characteristics were extracted from their medical records. Overall survival was calculated from the first resection surgery to death. The Karnofsky performance status (KPS) was determined as recorded or was retrospectively estimated from information obtained from the clinical chart by three neurosurgeons (Y.N., Y.M., and S.S.) who performed surgery on the patients. RPA classification of each patient was performed using published criteria [1]. Preoperative status, including performance status and RPA, was evaluated at the time of surgery, while postoperative status was evaluated approximately 1 month after surgery. The performance status and RPA class of patients who died within 1 month after surgery were recorded as 0 and III, respectively. Information regarding the RPA class and status of extracranial malignancy was not available for 1 case.

The cause of death was determined by clinical evaluation. Neurological deaths were defined as cases with neurological deterioration and stable extracranial disease as well as cases with apparent fatal progression of intracranial lesions or leptomeningeal metastases (LMM) regardless of systemic conditions.

The analysis in this study was approved by the local institutional review board (reference no. NCC16-066).

Treatment

Our basic surgical indications for brain metastases were described in a previous report [10]. Surgical candidates included patients with the following characteristics: (1) a post-surgery life expectancy of 6 months or more based on information from medical oncologists, (2) no clinical symptoms or apparent radiological findings indicating LMM, and (3) single metastases measuring $\geqq$3 cm, or multiple or smaller tumors associated with severe neurological symptoms such as cerebellar metastases. In principle, adjuvant radiotherapy usually began 8 days after surgery. Adjuvant stereotactic radiosurgery (SRS) or stereotactic radiotherapy (SRT) was undergone only for the treatment of the surgical remnant or unresected lesion(s) in patients with multiple metastases. After brain metastases were controlled, patients received further systemic therapy or best supportive care (BSC) according to decisions made by medical oncologists.

A total of 37 patients received RT prior to surgery. In patients who experienced tumor recurrence after radiotherapy, surgical indication was judged via discussion with senior radiologists.

Early death

Early death was defined as death within 6 months after the first surgery for brain metastases, and the clinical profiles between the early death group and the non-early death group were compared. This definition is based on a comparison between the outcome of whole brain radiation therapy (WBRT) and surgery. The median survival time (MST) after WBRT alone is approximately 6 months [11–13]; therefore, if surgery confers a survival benefit, it should extend this time period.

Statistical analysis

Statistical analysis was performed using JMP version 10 (SAS Institute, Cary, NC, USA). The data for survival time were analyzed using the Kaplan–Meier method. A P value below 0.05 was considered statistically significant.

Results

Analysis for all cases

When all cases were analyzed, the median follow-up, MST, 1-year overall survival rate, and 5-year overall survival rate were 11.2, 12.4 months, 52, and 12 %, respectively. The 3 and 6-month overall survival rates were 89 and 75 %, respectively. When patients were divided according to preoperative RPA class, we determined that MST was 21.8 months for class I (59 cases, 22 %), 12.4 months for class II (148 cases, 56 %), and 6.5 months for class III (56 cases, 21 %) (Fig. 1a). When we reevaluated the data using postoperative RPA classification, MST was 20.8 months for class I (66 cases, 25 %), 11.2 months for class II (176 cases, 67 %), and 4.3 months for class III (21 cases, 8 %) (Fig. 1b). Both of pre- and postoperative RPA class were significantly related with survival ($P < 0.0001$, log-rank test). The relationships between preoperative and postoperative RPA class are shown in Supplementary Table 1.

KPS improved in 53 %, was unchanged in 40 %, and worsened in 7 % of all cases after surgery. Surgical complications were observed in 20 cases (7.6 %) including 8 instances of neurological deterioration due to surgical

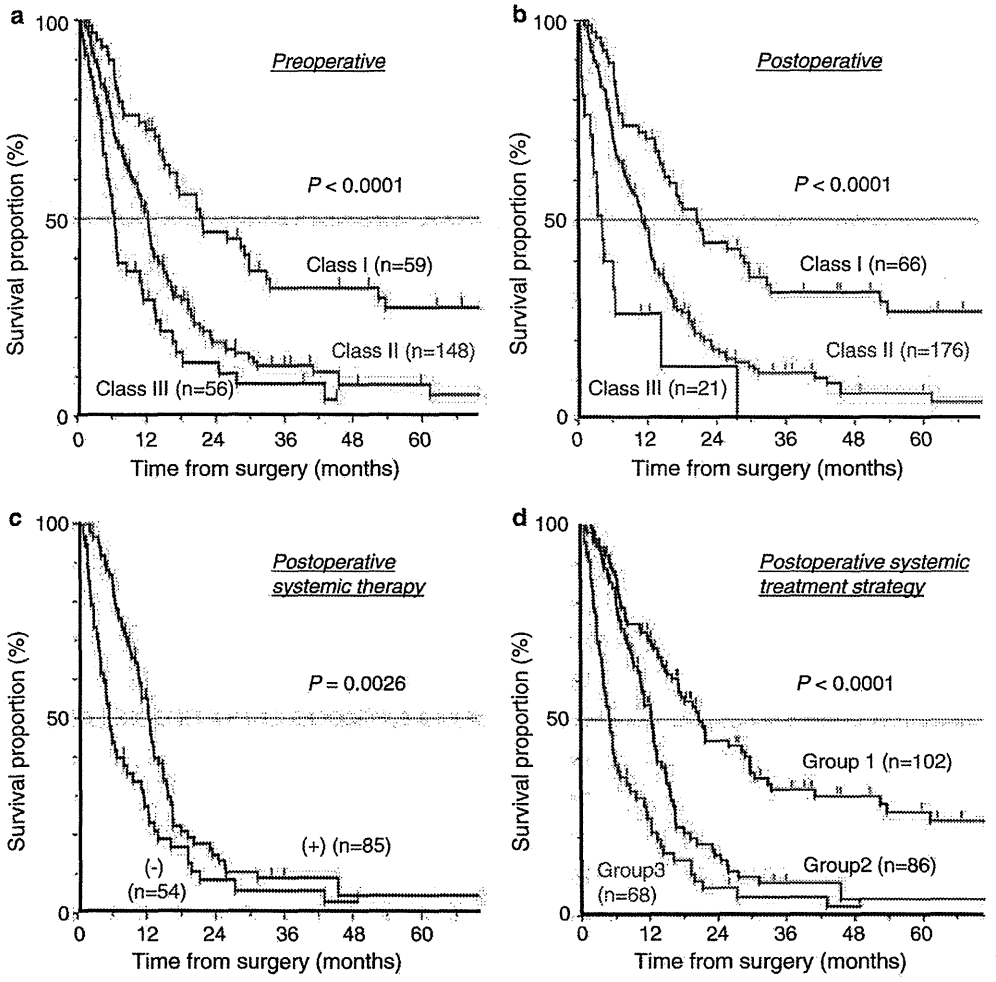

Fig. 1 Survival analysis. **a** Survival curves according to preoperative RPA class. MST was 21.8 months for class I, 12.4 months for class II, and 6.5 months for class III. **b** Survival curves according to postoperative RPA class. MST was 20.8 months for class I, 11.2 months for class II, and 4.3 months for class III. **c** Survival curves according to type of adjuvant therapy in patients with high KPS (70 or more) and uncontrolled extracranial malignancies. MST was 12.5 months for the systemic therapy (+) group and 5.6 months for the systemic therapy (−) group. **d** Survival curves according to postoperative systemic therapy. Group 1 consisted of patients without systemic disease, group 2 consisted of patients undergoing systemic therapy for uncontrolled extracranial disease, and group 3 consisted of patients who had extracranial disease but did not receive systemic therapy. MST was 20.8 months for group 1, 12.4 months for group 2, and 5.1 months for group 3

manipulation, 3 cerebral infarctions, 2 cases requiring evacuation of intraparenchymal hemorrhage, 1 case requiring evacuation of epidural hematoma, 1 case treated conservatively for intraparenchymal hemorrhage, 1 case requiring ventricular drainage for obstructive hydrocephalus, 1 instance of pulmonary embolism, 1 instance of surgical site infection, 1 sudden cardiopulmonary arrest, and 1 instance of vocal paralysis related to intubation. A permanent neurological deficit occurred in 11 (4.2 %) patients, but did not lead to early death in any case. Four patients (1.5 %) succumbed to surgery-related death (i.e., death within 30 days after surgery). Of these, two died of advanced systemic diseases 22 and 30 days after surgery, respectively. The other patients experienced neurological death: 1 died of LMM 23 days after surgery, while the other died of brainstem infarction 17 days after surgery for frontal lobe metastases.

Clinical characteristics of the early death group

A total of 62 patients (23 %) were included in the early death group. The early death rates were 10, 22, and 41 % in preoperative RPA class I, II, and III patients. When patients were divided according to postoperative RPA class, the

Table 1 Patient characteristics

	Total	Early death	Non-early death	*P* value[a]
Patients no.	264	62	202	
Multiple BM	67	24	43	0.0058
Infra-tentorial lesions	79	18	61	0.86
Age 65 or more	82	16	66	0.31
Preoperative KPS <70	57	24	33	0.0002
Postoperative KPS <70	22	13	9	<0.0001
ECM and/or uncontrolled primary lesion[b]	161	50	111	0.0003
Preoperative RPA[b]				0.0059[c]
I	59	6	53	
II	148	33	115	
III	56	23	33	
Postoperative RPA[b]				0.0041[c]
I	66	7	59	
II	176	43	133	
III	21	12	9	
Primary cancer				
Lung	102	24	78	
Breast	48	11	37	
GI	46	14	32	
Malignant melanoma	13	5	8	
Renal	8	2	6	
Others	47	6	41	
GTR	232	53	179	0.51
Any RT prior to surgery	37	11	26	0.33
Adjuvant RT(+)	216	46	170	0.075
Systemic therapy after operation for BM				
(+)	119	16	103	<0.0001
(−)	129	46	83	

BM brain metastases, *ECM* extra-cranial metastases, *GI* gastrointestinal, *GTR* gross total removal, *KPS* Karnofsky performance status, *RPA* recursive partitioning analysis, *RT* radiation therapy, *WBRT* whole brain radiation therapy

[a] Pearson's Chi square test

[b] Data of one case was absent

[c] Analyzing with dividing into RPA I and II-III

early death rates were 11, 24, and 57 % in class I, II, and III patients, respectively.

Table 1 shows the results of univariate analysis of data from the early death group and the non-early death group. The early death group contained a significantly higher ratio of patients with multiple brain metastases, KPS <70, uncontrolled primary cancers, and advanced RPA (II or III). The distribution of primary cancers did not differ significantly between these 2 groups. Fewer patients received systemic therapy after the resection of brain metastases in the early death group than in the non-early death group (26 vs. 55 %).

Table 2 Multiple logistic regression analysis for early death

	Odds ratio	*P* value
Postoperative systemic therapy (−)	4.91	<0.0001
Uncontrolled extra-cranial malignancy (+)	5.22	0.0022
Postoperative poorer KPS (<70)	3.61	0.041
Multiple brain metastases	(2.04)	0.051
Preoperative poorer KPS (<70)	(1.84)	0.18
Preoperative advanced RPA (class II or III)	(0.79)	0.84
Postoperative advanced RPA (class II or III)	(0.96)	0.98
Adjuvant radiotherapy (not performed)	(1.69)	0.21

KPS Karnofsky performance status, *RPA* recursive partitioning analysis

Multivariate logistic regression analysis was performed to identify which factors were most closely related with early death. Only clinical factors with $P < 0.1$ in univariate analysis (as described above) were used for this analysis. As shown in Table 2, uncontrolled primary tumors or extracranial metastases, lack of postoperative systemic therapy, and a postoperative decrease in KPS (<70) were significantly related to early death.

The impact of postoperative systemic therapy on the survival of patients with uncontrolled extracranial disease

The impact of treatment strategy on survival was further analyzed because postoperative systemic therapy was significantly related with early death in the univariate and multivariate analyses described above. Survival analysis using the Kaplan–Meier method did not reveal a difference in survival between patients in the systemic therapy (+) group (119 cases) and the (−) group (129 cases) (12.9 vs. 10.7 months; $P = 0.68$, log-rank test). Because systemic therapy is not usually administered to patients with poor performance status or without extra-cranial malignancies, we performed a further analysis including only patients with uncontrolled extracranial malignancies and those with a postoperative KPS of 70 or more. Based on this analysis, the MST was significantly longer in the systemic therapy (+) group (85 cases) than in the systemic therapy (−) group (54 cases) (12.5 vs. 5.6 months; $P = 0.0026$, log-rank test) (Fig. 1c).

The impact of postoperative treatment strategy on survival

All patients were divided into 3 groups according to treatment course after surgery for brain metastases: group 1

(102 cases) included patients without systemic disease, group 2 (89 cases) included patients who underwent systemic therapy for uncontrolled extracranial disease, and group 3 (65 cases) included patients who had extracranial disease but did not receive systemic therapy. Group 3 patients were treated with best supportive care. The MSTs of groups 1, 2, and 3 were 20.8, 12.4, and 5.1 months, respectively, and the difference among the groups was significant ($P < 0.0001$, log-rank test) (Fig. 1d). The early death rate was 12 % in group 1, 16 % in group 2 and 55 % in group 3, and the early death rate of group 3 was significantly higher than that of the other groups ($P < 0.0001$, Pearson's Chi square test).

Cause of death

Data regarding cause of death was available for 55 of the early death cases. Twenty patients (32 %) died from neurological causes, while 35 patients (56 %) died from systemic diseases. Thirteen of the neurological deaths were attributed to LMM. The adjuvant radiation therapies used in LMM cases were WBRT in 5 and local brain radiation therapy in 3 cases. Five cases did not receive either therapy. Other neurological deaths were due to progression of brain metastases after RT (6 cases) and brain stem infarction (1 case).

Postoperative status and survival time in preoperative RPA class III patients

Patients assessed as preoperative RPA class III ($n = 56$) typically have shorter survival times; therefore, the clinical courses of these patients were further analyzed in order to evaluate the potential treatment benefit. Of these patients, 8 (14 %), 31 (55 %), and 17 (30 %) were postoperative RPA class I, II, and III, respectively. When patients were divided according to postoperative RPA class, MST was 13.6, 6.5, and 3.6 months in class I, II, and III patients, respectively. MST was significantly longer in patients who experienced an improvement in postoperative RPA class ($n = 39$) compared with patients who remained in class III ($n = 17$) (6.9 vs. 3.6 months; $P = 0.019$, log-rank test). KPS was improved in 43 (77 %), unchanged in 10 (18 %), and worsened in 3 (5.4 %) preoperative RPA class III cases after surgery.

We further analyzed the cases showing RPA class III preoperatively but better RPA class postoperatively (I, 8 cases; II 31 cases) in order to discuss the operative indication for preoperative RPA class III patients (Supplementary Table 1). Twelve cases (31 %) of this cohort (39 cases) succumbed to early death after surgery, and their postoperative RPA class was I in one and II in 11. The causes of their early death were mainly consisted of systemic death; systemic disease in 8 cases, leptomeningeal metastasis in 2 cases and unknown in 2 cases. To identify what factor contributed to the early death in this cohort (39 cases), the postoperative treatment strategy was compared between the early death cases (12 cases) and the non-early death cases (27 cases). Eight of the 12 early death cases received best supportive care while 7 of the 25 non-early death cases (2 cases lacked the data) did. Thus, lack of postoperative systemic therapy was also statistically related with the early death in this cohort despite improvement in RPA class (8/12 vs. 7/25; $P = 0.025$, Pearson's Chi square test).

Discussion

In this study, we reviewed a surgical series from a single center and focused on the clinical characteristics of cases with poorer prognosis. Comparing with the recent studies presenting their surgical outcome, our series showed the comparable survival time [3, 6, 7, 9] according to RPA class and the comparable complication rate (7.6 vs. 4.5–14 %) despite the high ratio of RPA class III (21 vs. 5.7–6.8 %) [6, 14, 15]. We showed that postoperative treatment strategy and performance status were the significant factors for early death in multivariate analysis.

Systemic therapy after surgery was previously reported as being significantly related to survival time, but this was contradicted by the result in multivariate analysis [6]. This result simply seems to reflect the bias of the analysis: systemic therapy is usually avoided in patients with poorer performance status or patients without uncontrolled extracranial malignancy. We further analyzed only patients with favorable postoperative KPS scores and uncontrolled extracranial malignancies to ensure that we were only analyzing patients who truly needed further treatment for primary cancer. We showed that postoperative systemic therapy had a significant effect on survival in this population (Fig. 1c). Similarly, multivariate analysis showed that a lack of postoperative systemic therapy was a significant factor for early death, which was mainly analyzed in this study (Table 2). Thus, the treatment strategy for extracranial malignancies should be considered when determining operative indication, and this is supported by the results described in Fig. 1d. In other words, patients who cannot undergo chemotherapy (e.g., due to multidrug resistance to systemic therapy) are at high risk of early death after surgery. We also subjected our cohort to further analysis for survival by dividing three groups time according to the operative period (2000–2003, 2004–2007 and 2008–2011), but the difference in OS or early death rate was not apparent (data not shown). Despite the recent advances in systemic therapeutic agents, brain metastases

Table 3 Review of previous clinical studies: cause of death

Treatment		Pt no.	MST (months)	Neurological death (%)[c]	Systemic death[c]	Unknown[c]
Hashimoto et al. [17]	Surgery + WBRT	66	11.5	37	35 %	31 %
	Surgery + LBRT	64	9.7	36	36 %	29 %
Muacevic et al.[a] [18]	Surgery + WBRT	33	9.5	29	53 %	N.A.
	SRS	31	10.3	11	53 %	N.A.
Aoyama et al. [19]	WBRT + SRS	65	7.5	19	N.A.	N.A.
	SRS alone	67	8.0	23	N.A.	N.A.
Manon et al. [20]	SRS	31	8.3	19	30 %	16 %
Serizawa et al. [21]	SRS	521	9.0	18	N.A.	N.A.
Jawahar et al. [22]	SRS	44	7.0	25	36 %	39 %
Andrews et al. [11]	WBRT + SRS	137	6.5	28	62 %	9 %
	WBRT alone	149	5.7	31	64 %	5 %
Petrovich et al. [23]	SRS for MM	231	8	42	50 %	8 %
	SRS for others	227	6–17[b]	23	70 %	7 %
Agboola et al. [5]	Surgery + RT	125	9.5	25	37 %	6 %
Mintz et al. [13]	Surgery + WBRT	41	5.6	15	46 %	5 %
	WBRT	43	6.3	28	35 %	0 %
Wronski et al. [24]	Surgery ± WBRT	231	13	39	30 %	12 %
Bindal et al. [25]	Surgery ± WBRT	82				
	Multiple lesions	56	10	36	32 %	23 %
	Single lesion	30	14	25	45 %	15 %
Vecht et al. [16]	Surgery + WBRT	32	10	32	N.A.	N.A.
	WBRT	31	6	33	N.A.	N.A.

LBRT local brain radiation therapy, *MM* malignant melanoma, *MST* median survival time, *RT* radiation therapy, *SRS* stereotactic radiosurgery, *WBRT* whole brain radiation therapy

[a] The ratio was evaluated with 1-year rate

[b] The ratio was described in each cancer

[c] Deaths of combined cause of systemic and neurological were not included in any groups. When unknown cause were excluded from analysis in the original articles, the ratios were re-estimated including deaths of unknown causes

may arise after acquiring drug resistance even for newly developed agents, and the survival after brain metastases might depend largely on whether further systemic therapy can be available or not.

One of the challenges in our study was evaluating both preoperative and postoperative status. The prognostic significance of pre- and postoperative RPA class was previously analyzed, and the multivariate analysis showed that only preoperative RPA was significant [9]. This observation was, however, based simply on the analysis of survival time. Our analysis differed from the previous study because we evaluated the factor related to early death and specifically analyzed the group with the poorest prognosis: preoperative RPA class III patients. In the present study, postoperative RPA class was related to survival and a higher early death rate, and the early death rate was extremely high in preoperative RPA class III patients without postoperative improvement. Because RPA class III simply indicates a poor KPS score (<70), improvement in performance status is a significant factor for survival in preoperative RPA class III patients. Therefore, when determining the indications for surgery in preoperative RPA class III patients, it is important to consider whether surgery is likely to improve KPS. Patients who are not likely to experience an improvement in performance status are also not likely to obtain a survival benefit. However, it is important to remember that the postoperative treatment strategy is also significant factor for survival as shown in our analysis for RPA class III patients.

Finally, we analyzed the cause of death. Previous studies have reported a neurological death rate of 15–37 % after surgery for brain metastases [5, 11, 13, 16–25] (Table 3). Our results were in line with this, although one limitation of our study was that the cause of death was available only for early death cases. Of note, 21 % (13/62) of early death cases were attributed to LMM in this study. Recent large studies reported a 5–16 % incidence of LMM after surgical removal [14, 17, 26, 27]. Considering these results, LMM

appears to occur early after surgery and may be a significant cause of early death. An increased incidence of early death might be attributed to either (1) preoperative undiagnosed LMM without apparent radiological findings because of a lack of routine cerebrospinal fluid cytology [26] or (2) LMM caused by the surgery itself. In fact, several previous reports have shown an increased risk of LMM after surgery compared with SRS alone [14, 26–28]. In order to reduce early deaths due to LMM, adjuvant therapies will need to be developed. The protective effect of adjuvant radiation therapy for LMM remains controversial, and recent studies have failed to demonstrate this effect [14, 26]. Further studies are needed to clarify the efficacy of radiation therapy.

In summary, early death after resection of brain metastases can be attributed to neurologic factors and systemic factors. Of the neurological factors, LMM is a critical factor that is related to early death. Further studies exploring the prevention and treatment of LMM are necessary. Of the systemic factors, a poor performance status after surgery (rather than before surgery), uncontrolled extracranial malignancies, and a lack of systemic therapy after surgery are related to early death. The limitation of our retrospective study lies in the possibility of the bias derived from patient selection. Further analysis including non-surgically treated cases may confirm our observations. When making decisions regarding surgery for brain metastases, physicians should be aware of the importance of a systemic treatment strategy after surgery, while surgeons should recognize that a poor performance status deprives patients of QOL and a chance for systemic therapy. The role of surgery for brain metastases is not only to improve the QOL and prevent neurological death but also to give patients a chance for further systemic therapy.

Acknowledgments This work was supported in part by Grant-in-Aid for Scientific Research from the Ministry of Education, Science and Culture of Japan [No. 24592180 (YN) and 24659650 (HA)].

Conflict of interest The authors declare that they have no conflict of interest.

References

1. Gaspar L, Scott C, Rotman M, Asbell S, Phillips T, Wasserman T, McKenna WG, Byhardt R (1997) Recursive partitioning analysis (RPA) of prognostic factors in three Radiation Therapy Oncology Group (RTOG) brain metastases trials. Int J Radiat Oncol Biol Phys 37:745–751
2. Sperduto PW, Chao ST, Sneed PK, Luo X, Suh J, Roberge D, Bhatt A, Jensen AW, Brown PD, Shih H, Kirkpatrick J, Schwer A, Gaspar LE, Fiveash JB, Chiang V, Knisely J, Sperduto CM, Mehta M (2010) Diagnosis-specific prognostic factors, indexes, and treatment outcomes for patients with newly diagnosed brain metastases: a multi-institutional analysis of 4,259 patients. Int J Radiat Oncol Biol Phys 77:655–661. doi:10.1016/j.ijrobp.2009.08.025
3. Tendulkar RD, Liu SW, Barnett GH, Vogelbaum MA, Toms SA, Jin T, Suh JH (2006) RPA classification has prognostic significance for surgically resected single brain metastasis. Int J Radiat Oncol Biol Phys 66:810–817. doi:10.1016/j.ijrobp.2006.06.003
4. Golden DW, Lamborn KR, McDermott MW, Kunwar S, Wara WM, Nakamura JL, Sneed PK (2008) Prognostic factors and grading systems for overall survival in patients treated with radiosurgery for brain metastases: variation by primary site. J Neurosurg 109(Suppl):77–86. doi:10.3171/JNS/2008/109/12/S13
5. Agboola O, Benoit B, Cross P, Da Silva V, Esche B, Lesiuk H, Gonsalves C (1998) Prognostic factors derived from recursive partition analysis (RPA) of Radiation Therapy Oncology Group (RTOG) brain metastases trials applied to surgically resected and irradiated brain metastatic cases. Int J Radiat Oncol Biol Phys 42:155–159
6. Paek SH, Audu PB, Sperling MR, Cho J, Andrews DW (2005) Reevaluation of surgery for the treatment of brain metastases: review of 208 patients with single or multiple brain metastases treated at one institution with modern neurosurgical techniques. Neurosurgery 56:1021–1034 (discussion 1021–1034)
7. Nieder C, Astner ST, Andratschke NH, Marienhagen K (2011) Postoperative treatment and prognosis of patients with resected single brain metastasis: how useful are established prognostic scores? Clin Neurol Neurosurg 113:98–103. doi:10.1016/j.clineuro.2010.09.009
8. Chidel MA, Suh JH, Reddy CA, Chao ST, Lundbeck MF, Barnett GH (2000) Application of recursive partitioning analysis and evaluation of the use of whole brain radiation among patients treated with stereotactic radiosurgery for newly diagnosed brain metastases. Int J Radiat Oncol Biol Phys 47:993–999. doi:S0360-3016(00)00527-7
9. Schackert G, Lindner C, Petschke S, Leimert M, Kirsch M (2013) Retrospective study of 127 surgically treated patients with multiple brain metastases: indication, prognostic factors, and outcome. Acta Neurochirurg. doi:10.1007/s00701-012-1606-8
10. Narita Y, Shibui S (2009) Strategy of surgery and radiation therapy for brain metastases. Int J Clin Oncol Jpn Soc Clin Oncol 14:275–280. doi:10.1007/s10147-009-0917-0
11. Andrews DW, Scott CB, Sperduto PW, Flanders AE, Gaspar LE, Schell MC, Werner-Wasik M, Demas W, Ryu J, Bahary JP, Souhami L, Rotman M, Mehta MP, Curran WJ Jr (2004) Whole brain radiation therapy with or without stereotactic radiosurgery boost for patients with one to three brain metastases: phase III results of the RTOG 9508 randomised trial. Lancet 363:1665–1672. doi:10.1016/S0140-6736(04)16250-8
12. Datta R, Jawahar A, Ampil FL, Shi R, Nanda A, D'Agostino H (2004) Survival in relation to radiotherapeutic modality for brain metastasis: whole brain irradiation versus gamma knife radiosurgery. Am J Clin Oncol 27:420–424
13. Mintz AH, Kestle J, Rathbone MP, Gaspar L, Hugenholtz H, Fisher B, Duncan G, Skingley P, Foster G, Levine M (1996) A randomized trial to assess the efficacy of surgery in addition to radiotherapy in patients with a single cerebral metastasis. Cancer 78:1470–1476
14. Suki D, Hatiboglu MA, Patel AJ, Weinberg JS, Groves MD, Mahajan A, Sawaya R (2009) Comparative risk of leptomeningeal dissemination of cancer after surgery or stereotactic radiosurgery for a single supratentorial solid tumor metastasis. Neurosurgery 64:664–674. doi:10.1227/01.NEU.0000341535.53720.3E (discussion 674–666)
15. Lee CH, Kim DG, Kim JW, Han JH, Kim YH, Park CK, Kim CY, Paek SH, Jung HW (2013) The role of surgical resection in the

management of brain metastasis: a 17-year longitudinal study. Acta Neurochirurg. doi:10.1007/s00701-013-1619-y
16. Vecht CJ, Haaxma-Reiche H, Noordijk EM, Padberg GW, Voormolen JH, Hoekstra FH, Tans JT, Lambooij N, Metsaars JA, Wattendorff AR et al (1993) Treatment of single brain metastasis: radiotherapy alone or combined with neurosurgery? Ann Neurol 33:583–590. doi:10.1002/ana.410330605
17. Hashimoto K, Narita Y, Miyakita Y, Ohno M, Sumi M, Mayahara H, Kayama T, Shibui S (2011) Comparison of clinical outcomes of surgery followed by local brain radiotherapy and surgery followed by whole brain radiotherapy in patients with single brain metastasis: single-center retrospective analysis. Int J Radiat Oncol Biol Phys 81:e475–e480. doi:10.1016/j.ijrobp.2011.02.016
18. Muacevic A, Wowra B, Siefert A, Tonn JC, Steiger HJ, Kreth FW (2008) Microsurgery plus whole brain irradiation versus Gamma Knife surgery alone for treatment of single metastases to the brain: a randomized controlled multicentre phase III trial. J Neurooncol 87:299–307. doi:10.1007/s11060-007-9510-4
19. Aoyama H, Shirato H, Tago M, Nakagawa K, Toyoda T, Hatano K, Kenjyo M, Oya N, Hirota S, Shioura H, Kunieda E, Inomata T, Hayakawa K, Katoh N, Kobashi G (2006) Stereotactic radiosurgery plus whole-brain radiation therapy vs stereotactic radiosurgery alone for treatment of brain metastases: a randomized controlled trial. JAMA 295:2483–2491. doi:10.1001/jama.295.21.2483
20. Manon R, O'Neill A, Knisely J, Werner-Wasik M, Lazarus HM, Wagner H, Gilbert M, Mehta M (2005) Phase II trial of radiosurgery for one to three newly diagnosed brain metastases from renal cell carcinoma, melanoma, and sarcoma: an Eastern Cooperative Oncology Group study (E 6397). J Clin Oncol 23:8870–8876. doi:10.1200/JCO.2005.01.8747
21. Serizawa T, Saeki N, Higuchi Y, Ono J, Iuchi T, Nagano O, Yamaura A (2005) Gamma knife surgery for brain metastases: indications for and limitations of a local treatment protocol. Acta Neurochirurg 147:721–726. doi:10.1007/s00701-005-0540-4 (discussion 726)
22. Jawahar A, Matthew RE, Minagar A, Shukla D, Zhang JH, Willis BK, Ampil F, Nanda A (2004) Gamma knife surgery in the management of brain metastases from lung carcinoma: a retrospective analysis of survival, local tumor control, and freedom from new brain metastasis. J Neurosurg 100:842–847. doi:10.3171/jns.2004.100.5.0842
23. Petrovich Z, Yu C, Giannotta SL, O'Day S, Apuzzo ML (2002) Survival and pattern of failure in brain metastasis treated with stereotactic gamma knife radiosurgery. J Neurosurg 97:499–506. doi:10.3171/jns.2002.97.supplement5.0499
24. Wronski M, Arbit E, Burt M, Galicich JH (1995) Survival after surgical treatment of brain metastases from lung cancer: a follow-up study of 231 patients treated between 1976 and 1991. J Neurosurg 83:605–616. doi:10.3171/jns.1995.83.4.0605
25. Bindal RK, Sawaya R, Leavens ME, Lee JJ (1993) Surgical treatment of multiple brain metastases. J Neurosurg 79:210–216. doi:10.3171/jns.1993.79.2.0210
26. Ahn JH, Lee SH, Kim S, Joo J, Yoo H, Shin SH, Gwak HS (2012) Risk for leptomeningeal seeding after resection for brain metastases: implication of tumor location with mode of resection. J Neurosurg 116:984–993. doi:10.3171/2012.1.JNS111560
27. Suki D, Abouassi H, Patel AJ, Sawaya R, Weinberg JS, Groves MD (2008) Comparative risk of leptomeningeal disease after resection or stereotactic radiosurgery for solid tumor metastasis to the posterior fossa. J Neurosurg 108:248–257. doi:10.3171/JNS/2008/108/2/0248
28. van der Ree TC, Dippel DW, Avezaat CJ, Sillevis Smitt PA, Vecht CJ, van den Bent MJ (1999) Leptomeningeal metastasis after surgical resection of brain metastases. J Neurol Neurosurg Psychiatry 66:225–227

Surgical Neurology International

OPEN ACCESS

For entire Editorial Board visit : http://www.surgicalneurologyint.com

Editor: James I. Ausman, MD, PhD University of California, Los Angeles, CA, USA

Original Article

Characteristics of brain metastases from esophageal carcinoma

Takahiro Yamamoto[1,2], Jun-ichiro Kuroda[1], Tatsuya Takezaki[1], Naoki Shinojima[1], Takuichiro Hide[1], Keishi Makino[1], Hideo Nakamura[1], Shigetoshi Yano[1], Toru Nishi[2], Jun-ichi Kuratsu[1]

[1]Departments of Neurosurgery, Faculty of Life Sciences, Kumamoto University School of Medicine, 1-1-1, Honjo, Kumamoto 860 - 8556, [2]Saiseikai Kumamoto Hospital, 1-3-5, Chikami, Kumamoto 861- 4193, Japan

E-mail: *Takahiro Yamamoto - tyamamoto0915@yahoo.co.jp; Jun-ichiro Kuroda - jukuroda@kumamoto-u.ac.jp; Tatsuya Takezaki - ttakezaki@mac.com; Naoki Shinojima - nshinojima@fc.kuh.kumamoto-u.ac.jp; Takuichiro Hide - thide@fc.kuh.kumamoto-u.ac.jp; Keishi Makino - kmakino@fc.kuh.kumamoto-u.ac.jp; Hideo Nakamura - hnakamur@fc.kuh.kumamoto-u.ac.jp; Shigetoshi Yano - yanos@kumamoto-u.ac.jp; Toru Nishi - toru-nishi@saiseikaikumamoto.jp; Jun-ichi Kuratsu - jkuratsu@kumamoto-u.ac.jp
*Corresponding author

Received: 25 July 14 Accepted: 30 July 14 Published: 22 September 14

This article may be cited as:
Yamamoto T, Kuroda J, Takezaki T, Shinojima N, Hide T, Makino K, *et al*. Characteristics of brain metastases from esophageal carcinoma. Surg Neurol Int 2014;5:137.
Available FREE in open access from: http://www.surgicalneurologyint.com/text.asp?2014/5/1/137/141468

Abstract

Background: Esophageal carcinoma (EC) is a major malignancy with a poor prognosis. Although esophageal cancers rarely metastasize to the brain, the number of patients diagnosed with brain metastases (BM) from EC is steadily increasing. Therefore, the risk factors for BM from EC should be known. Here we reviewed our experiences and the previous literature regarding BM from EC.

Methods: Between 2000 and 2013, we retrospectively reviewed the clinical features and neurological findings of 19 patients diagnosed with and treated for BM from EC to determine the clinical risk factors and features.

Results: In all patients, the lesions were partially or completed located in the thoracic esophagus, and the average size of the EC lesion at diagnosis was 5.8 ± 2.9 cm, which was smaller than the previously reported size of EC lesions accompanied by BM. Patients without lung metastases were more common than those with lung metastases. The lesions in the 13 patients included squamous cell carcinoma (SqCC) in 9 (69.2%) and small cell carcinoma (SmCC) in 3 (23.0%). Six patients were not examined. Although there was no trend toward a higher incidence of BM in patients with adenocarcinoma and SqCC, this trend was observed in patients with SmCC. Excluding a single patient with SmCC, all patients had beyond stage III disease at EC diagnosis.

Conclusions: Our study suggests that BM can occur in patients with EC lesions smaller than those previously reported; moreover, SmCC may be a risk factor for BM from EC.

Key Words: Adenocarcinoma, brain metastases, esophageal carcinoma, small cell carcinoma, squamous cell carcinoma

Access this article online

Website: www.surgicalneurologyint.com

DOI: 10.4103/2152-7806.141468

Quick Response Code:

INTRODUCTION

Esophageal carcinoma (EC) is a major malignancy with a poor prognosis and a 5-year survival rate of 23%.[22] According to the comprehensive registry of EC in Japan, EC often develops in the 7th decade in males, with a male-to-female ratio of approximately 7:1.[11] EC frequently metastasizes to the lymph nodes, liver, lung, and bone, but

rarely to the brain; the incidence of brain metastases (BM) from EC is approximately 0.6-1.5%.[11,16,22,23] Therefore, it is a rare occurrence, with as few as 150 cases reported worldwide [Table 1].[1-7,9,12-14,16-22] However, the number of patients diagnosed with BM from EC is increasing, probably because of advances in diagnostic imaging and treatment of the primary EC lesion.[18,21] Therefore, there has been a steady increase in the number of clinical reports of BM from EC, with well-described treatments and outcomes in particular.[11-13,16,18,22,23] Till date, however, there has been insufficient discussion of the clinical risk factors and features of BM from EC. Therefore, we reviewed our clinical experiences together with the existing literature to evaluate recent trends in the occurrence of BM in patients with EC.

MATERIALS AND METHODS

Between 2000 and 2013, 19 patients with BM from EC were diagnosed and treated at Kumamoto University Hospital and Saiseikai Kumamoto Hospital in Kumamoto City in southern Japan. All patients with BM were diagnosed by computed tomography (CT) or magnetic resonance imaging (MRI). To determine the clinical risk factors and features of BM in patients with EC, we retrospectively reviewed their clinical features and neurological findings. Specifically, the following information was collected: Patient age and sex, time from EC diagnosis to BM occurrence, EC size, EC stage at diagnosis, treatment, EC location, BM location and imaging characteristics, neurological symptoms, histology, concurrent metastatic sites, and survival data. Time from EC diagnosis to BM occurrence was actuarially calculated using the Kaplan-Meier method. A probability level of 0.05 was set for statistical significance. Statistical analysis was performed using StatMate III, Version 3.19 (ATMS, Tokyo, Japan).

Table 1: Published reports of brain metastases (BM) from esophageal carcinoma (EC)[1, 3-19]

Syudy	Year	Patients with BM
Appelqvist	1975	1
Bosch *et al.*	1979	1
Mandard *et al.*	1981	5
Anderson and Lad	1982	1
Sons and Borchard	1984	3
Chan *et al.*	1986	2
Kaneko *et al.*	1991	4
Gabrielsen *et al.*	1995	12
Quint *et al.*	1995	3
Takeshima *et al.*	2001	8
Ogawa *et al.*	2001	36
Weinberg *et al.*	2003	27
Almasi *et al.*	2004	1
Yoshida *et al.*	2007	17
Agrawal *et al.*	2009	1
Kanemoto *et al.*	2011	12
Smith and Miller	2011	7
Song *et al.*	2014	26
Present study	2014	19

BM from EC is a rare occurrence, with approximately 150 cases reported worldwide
EC: Esophageal carcinoma, BM; Brain metastases

RESULTS

Table 2 provides the clinical summary of all 19 patients. Table 3 summarizes the EC-related clinical data and characteristics. The average age at EC diagnosis was 65.5 ± 6.9 years (range 52-78 years), and the male-to-female ratio was 18:1.

The average EC size at diagnosis was 5.8 ± 2.9 cm in the 15 patients whose size data were collected. EC location ranged from cervical esophagus (Ce) to abdominal esophagus (Ae). The data on EC location were collected in 17 patients. EC that was partly or completely located in the middle thoracic esophagus (Mt) was the most common (12/17 patients), and the lesions were partly or completely located in the thoracic esophagus (Te) in all patients. In the 15 patients whose staging data were collected, EC at diagnosis was stage IV in 10 patients, stage III in 4 patients, and stage II in 1 patient; therefore, excluding 1 patient with small cell carcinoma (SmCC), all patients had beyond stage III disease.

The clinical data and characteristics of BM in the 19 patients are summarized in Table 4. The median time from EC diagnosis to BM occurrence was 7.0 months (range - 4 to 36 months. Time from EC diagnosis to BM occurrence was statistically significant, regardless of whether or not surgery was performed for EC [HR, 0.31 (0.038, 0.60); $P = 0.007$]. At diagnosis, 8 patients were asymptomatic and 11 had various neurological symptoms, including hemiplegia, seizure, visual disturbance, memory disturbance, and aphasia. Multiple BM lesions were found in eight patients. Among these, one patient had multiple metastases throughout the brain and the remaining seven had a total of 28 lesions: 9 each in the frontal and parietal lobes, 4 in the occipital lobe, 3 in the cranium, 2 each in the cerebellum and temporal lobe, and 1 in the corpus callosum. With regard to the features of BM on CT and/or MRI, 6 of 19 (31.5%) patients exhibited a cystic mass with an enhanced rim, 11 of 19 (57.8%) patients exhibited a solid mass with necrosis, and 2 of 19 (10.5%) patients exhibited a mass with bone destruction. Surgical resection of BM and/or EC was performed in 13 patients. Histological examination for these 13 patients revealed squamous cell carcinoma (SqCC) in 9 (69.2%), SmCC in 3 (23.0%), and basal cell carcinoma in 1 (7.6%). Six patients were without surgical resection and histological examination. Of note, the proportion of patients without lung metastasis was higher (57.8%) than that of patients

Table 2: Summary of the 19 patients with brain metastases from esophageal carcinoma (EC)

Age/ sex	Histology	Location of EC	Size of EC (cm)	Time from EC	Neurological symptoms	Lung metastases	Outcome (months)
67/M	SqCC	Te (Ut, Lt)	4	1Y, 11M	No symptoms	Yes	Died (8)
68/M	SmCC	Te (Mt)	2	2Y	No symptoms	Yes	-
67/M	SqCC	Te (Ut-Mt)	6	2Y	Convulsion	Yes	Died (18)
67/M	SqCC	Te (Lt)	6	3Y	Hemiplegia	No	Died (12)
68/F	SqCC	Te (Mt-Lt)	3	4M before	Memory disturbance	No	Died (12)
73/M	SqCC	Ce-Te (Mt)	7	6M	Hemiplegia	No	Died (2)
72/M	SqCC	Te (Mt-Lt)	6	1Y, 10M	No symptoms	No	Died (2)
59/M	-	Te (Mt)-Ae	5	1M	No symptoms	Yes	-
58/M	SqCC	Ce-Te (Ut)	5	3M	No symptoms	No	Died (2)
60/M	-	Te (Mt)-Ae	13	Same time	Hemiplegia, aphasia	No	Died (3)
60/M	-	Te (Mt), Lt	5	Same time	Hemianopsia	Yes	Died (4)
52/M	BasalCC	Te (Mt)	-	1Y	Disturbance of consciousness, hemianopsia	Yes	Died (34)
66/M	SmCC	-	-	4Y	Headache	Yes	Died (11)
69/M	SqCC	Te (Ut-Mt)	-	2M	Headache	No	-
52/M	-	-	-	3Y	No symptoms	No	-
70/M	-	Te (Mt)	3	Same time	No symptoms	No	Died (1)
71/M	SqCC	Te (Mt-Lt)	10	2Y	Headache, hemiplegia	No	Died (17)
69/M	-	Te (Lt)-Ae	9	7M	No symptoms	Yes	Alive (3)
78/M	SmCC	Te (Lt)	4	6M	Convulsion	No	Alive (1)

M: Male, F: Female, SqCC: Squamous cell carcinoma, SmCC: Small cell carcinoma, Ce: Cervical esophagus, Te: Thoracic esophagus, Ut: Upper thoracic esophagus, Mt: Middle thoracic esophagus, Lt: Lower thoracic esophagus, Ae: Abdominal esophagus, EC: Esophageal carcinoma

with lung metastasis. The survival period from diagnosis in the 13 patients whose survival data were collected ranged from 1 to 34 (average 9.7 ± 9.4) months.

DISCUSSION

According to the comprehensive registry of EC in Japan, EC progresses in 2% males and 0.4% females.[11] There are significant racial variations in the histological types of EC. According to the study of Chalasani *et al.*, SqCC was predominant (92%) while adenocarcinoma was rare among black patients. On the other hand, adenocarcinoma was more common (66%) than SqCC (32%) among white patients.[8] With regard to the histological type of primary EC in the Japanese population, SqCC is more common (86.9%) than adenocarcinoma (4.3%).[11] In a study by Weinberg *et al.*, histology did not appear to be a risk factor for BM, and among the patients with BM in that study, 82% had adenocarcinoma and 7% had SqCC.[22] Although Gabrielsen *et al.* reported that adenocarcinomas were more prone to metastasize to the brain compared with SqCC, their data were not significant ($P = 0.16$).[9] In contrast, there were no cases of adenocarcinoma in the present study; SqCC accounted for 9 of the 13 patients (69.2% BM cases), while SmCC and basal cell carcinoma accounted for 3 (23% BM cases) and 1 (7.6% BM cases) of the 13 patients, respectively. According to the comprehensive registry of EC in Japan, where SqCC occurs in 87.5% patients and adenocarcinoma in 4.3%, there is no trend toward a higher incidence of BM with adenocarcinoma or SqCC.[11] The proportion of patients with SmCC in our study was higher than that of EC in Japan, suggesting that SmCC is a specific risk factor for BM from EC. Further research is required to confirm this assertion. The features of BM on CT and/or MRI were not significantly correlated with histology (OR, 2.0; $P = 0.85$). However, compared with BM from lung cancer (cystic, 15%; solid, 85%), BM from EC show a greater tendency to become cystic masses with necrosis.[15]

Although it is well known that EC rarely metastasizes to the brain, the number of patients diagnosed with BM from EC is increasing. Metastases are thought to occur via local invasion and hematogenous spread,[22] with the latter being the most likely mechanism for BM. Typically, lung metastasis is rarely found in patients with BM from EC. Indeed, of the 27 patients in the study by Weinberg *et al.*, 7 (26%) had lung metastases.[22] In our study, 8 of the 19 patients (42.1%) had lung metastases, probably because hematogenous spread to the brain occurred via the Batson venous plexus. The Batson venous plexus is a network of valveless veins that connect the systemic veins to the internal vertebral venous plexuses.[5] Because of their location and lack of valves, they are thought to be a route for the lesion to metastasize to the brain without metastasizing to the lungs.[16,22] In particular, because the esophagus contains the esophageal venous plexus, EC lesions are likely to metastasize to the brain through the Batson venous plexus. This is supported by

Table 3: Clinical data and characteristics of esophageal carcinoma (EC) in the 19 patients

Clinical data and characteristics (total number of patients)	Number of patients	(%)
Age at EC diagnosis		
Range	52-78 (years)	-
Average±SD	65.5±6.9 (years)	-
Sex		
Male	18	(94.7)
Female	1	(5.2)
Size of EC (n=15: No data in 4 patients)		
Range	2-13 (cm)	-
Average±SD	5.8±2.9 (cm)	-
Location of EC (n=17: No data in 2 patients)		
Ce	2	(11.7)
Te		
Ut	5	(29.4)
Mt	12	(70.5)
Lt	9	(52.9)
Ae	3	(17.6)
Stage of EC at the diagnosis (n=15: no data in 4 patients)		
Tumor staging		
0 -I	0	(0)
II	1	(6.6)
III	4	(26.6)
IV	10	(66.6)
TNM classification		
Tx	2	(13.3)
Tis-T1	0	(0)
T2	2	(13.3)
T3-T4	11	(73.3)
Nx	1	(6.6)
N0	1	(6.6)
N1	13	(86.6)
Mx	0	(0)
M0	5	(33.3)
M1	10	(66.6)
Treatment for EC		
S+R+C	6	(31.5)
R+C	6	(31.5)
S+C	1	(5.2)
S+R	1	(5.2)
R	1	(5.2)
C	1	(5.2)
BSC	3	(15.7)

Stage: using TNM classification, SD: Standard deviation, S: Surgery, R: Radiotherapy, C: Chemotherapy, BSC: Best supportive care, EC: Esophageal carcinoma

Table 4: Clinical data and characteristics of brain metastases (BM) in the 19 patients

Clinical data and characteristics (Total number of patients)	Number of patients	(%)
Time from EC diagnosis and BM occurrence		
Range	−4-36 (months)	-
Average±SD	14.2±15.0 (months)	-
Median	7	-
Neurological symptoms		
No symptoms	8	(42.1)
Hemiplegia	4	(21.0)
Headache	3	(15.7)
Visual disturbance	2	(10.5)
Seizure	2	(10.5)
Memory disturbance	1	(5.2)
Aphasia	1	(5.2)
Location of BM		
Brain		
Frontal	9	(50)
Parietal	9	(50)
Occipital	4	(22.2)
Temporal	2	(11.1)
Cerebellar	2	(11.1)
Corpus callosum	1	(5.6)
Cranium	3	(16.7)
Feature of BM on images		
Cystic mass with enhanced rim	6	(31.5)
Solid with central necrosis	11	(57.8)
Bone destruction	2	(10.5)
Treatment for BM		
S+R	5	(26.3)
R	8	(42.1)
S	3	(15.7)
BSC	3	(15.7)
Histological type of BM and/or EC (n=13: No data in 6 patients)		
Squamous cell carcinoma	9	(69.2)
Small cell carcinoma	3	(23.0)
Basal cell carcinoma	1	(7.6)
Other metastatic sites		
Without lung metastasis	11	(57.8)
With lung metastasis	8	(42.1)
With LN metastasis	12	(63.1)
Survival period from BM diagnosis (n=13: No data in 6 patients)		
Range	1-34 (month)	-
Average±SD	9.7±9.39 (month)	-
Median	8 (month)	-

BM: Brain metastasis, EC: Esophageal carcinoma, BSC: Best supportive care, LN: Lymph node, SD: Standard deviation

the fact that the thoracic esophagus, which lies in the region of the esophageal venous plexus, was the most common location for EC in our study. This phenomenon may account for the low rate of lung metastases in patients with BM from EC.

In the study by Ogawa *et al.*, the primary lesions were stage III or stage IV in 81% patients with BM.[16] Our